Supporting information

A $Cu_{0.76}Co_{2.24}O_4$/γ-$Cu_2(OH)_3Cl$ Composite Catalyst for Efficient Neutral Nitrate Reduction

Xian Liu[a,b], Min Wang[c*], Wenhao Yang[c], Zixuan Wei[c], Jian Yang[a,b*]

[a] College of Materials Science and Engineering, Nanjing Tech University, Nanjing, 211816, China.

[b] Jiangsu Collaborative Innovation Center for Advanced Inorganic Function Composites, Nanjing 211816, China.

[c] Shanghai Institute of Ceramics, Chinese Academy of Sciences, 1295 Ding-xi Road, Shanghai, 200050, P. R. China.

E-mail: yangjian1976@163.com, wangmin@mail.sic.ac.cn

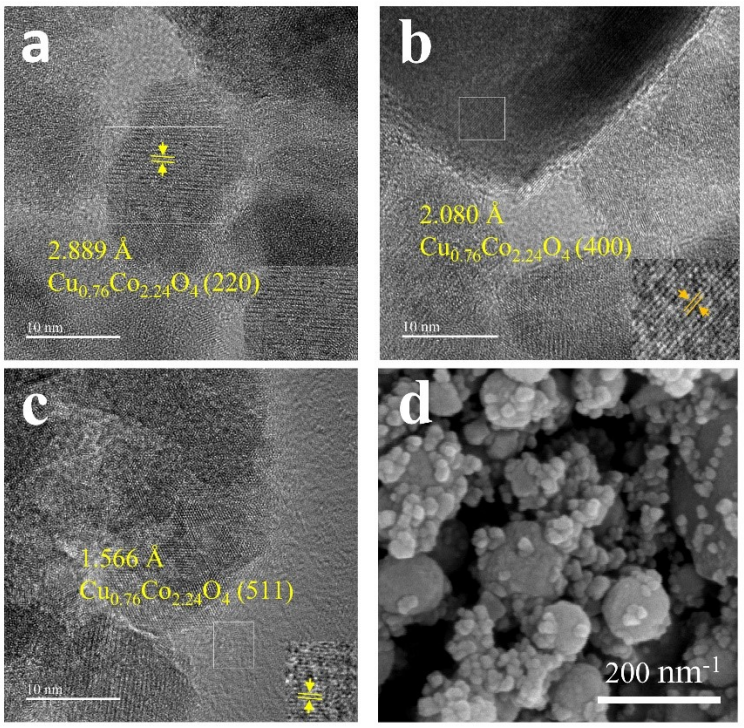

Figure S1. HRTEM(a-b) and SEM(d)images of CCOC.

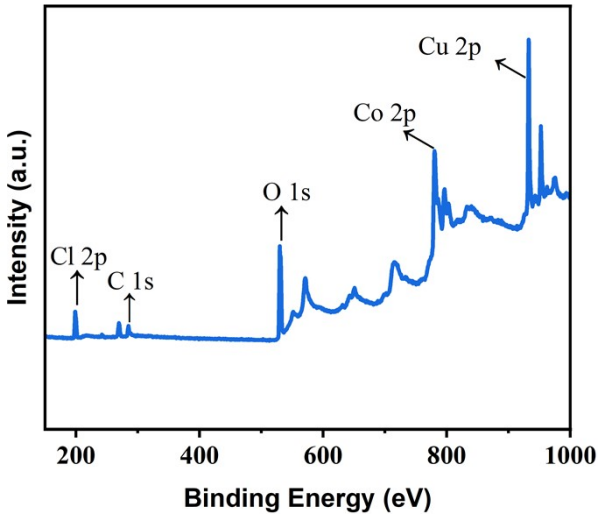

Figure S2. XPS survey spectrum of CCOC.

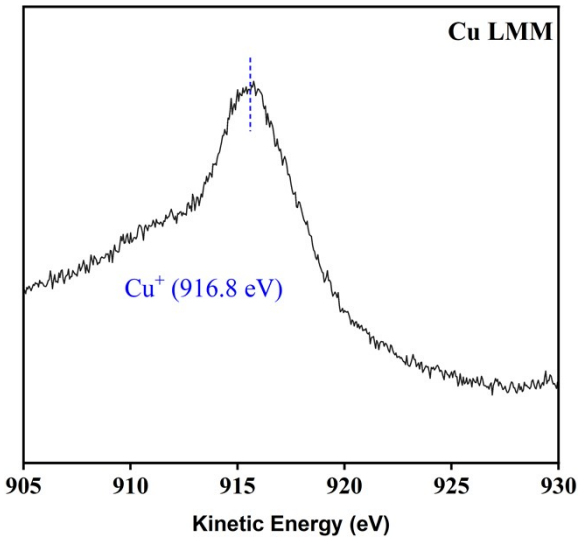

Figure S3. Cu LMM XPS spectrum of CCOC.

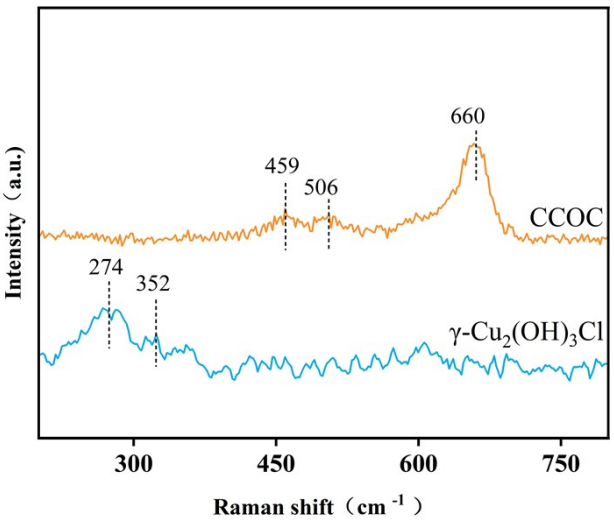

Figure S4. Raman spectra of CCOC and γ-$Cu_2(OH)_3Cl$. The bands at 274 and 352 cm^{-1} are attributed to bending vibration of Cu^{2+}. The bands at 459 cm^{-1} and 506 cm^{-1} are ascribed to bending vibration of Cu^{+}. The band at 660 cm^{-1} belongs to Co^{2+}/ Co^{3+}.

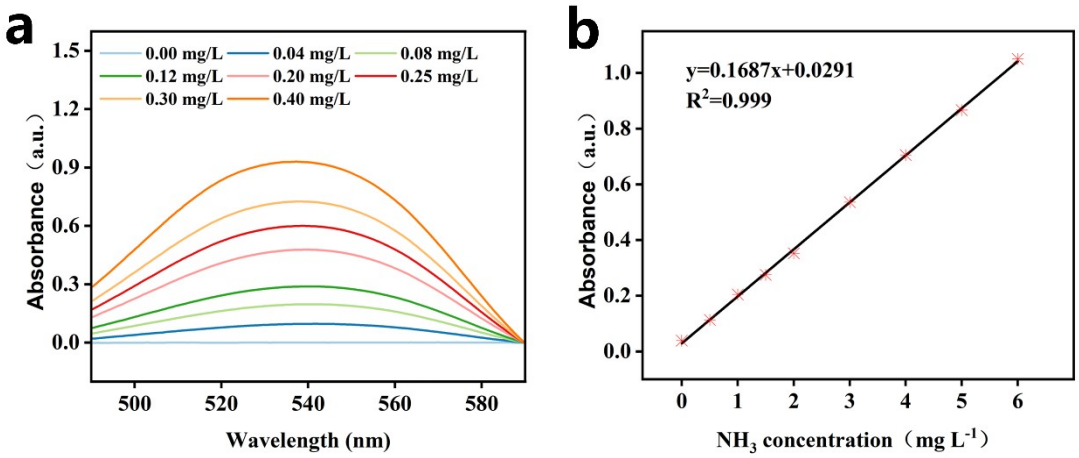

Figure S5. Calibration curve in 0.5 M Na_2SO_4 using ammonium chloride solutions of known concentration as standards. (a) Spectrophotometric UV-vis curves of salicylic acid after incubated for 1 hour and (b) calibration curve used for the estimation of NH_3 concentration. The absorbance at 655 nm was measured by a UV-Vis spectrophotometer, and the fitting curve shows good linear relation of absorbance with NH_3 concentration ($y = 0.1687x + 0.0291$, $R^2 = 0.999$).

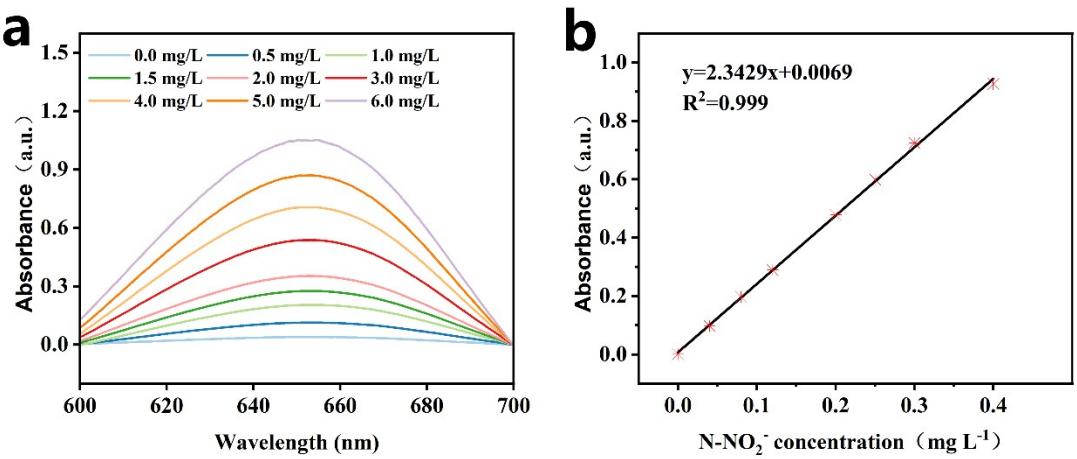

Figure S6. Calibration curve in 0.5 M Na_2SO_4 using potassium nitrite solutions of known concentration as standards. (a) Spectrophotometric UV-vis curves of salicylic acid after incubated for 20 minutes and (b) calibration curve used for the estimation of $N\text{-}NO_2^-$ concentration. The absorbance at 540 nm was measured by a UV-Vis spectrophotometer, and the fitting curve shows good linear relation of absorbance with $N\text{-}NO_2^-$ concentration ($y = 2.3429x + 0.0069$, $R^2 = 0.999$).

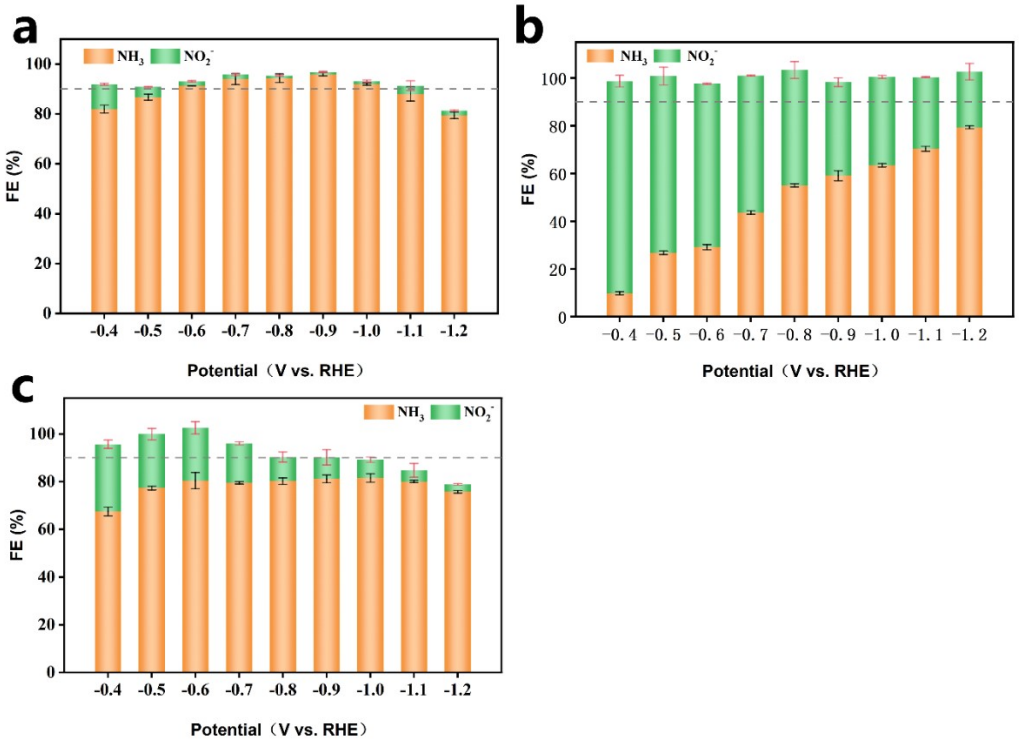

Figure S7. FE of NH_3 and NO_2^- at different applied potentials on CCOC(a), γ-$Cu_2(OH)_3Cl$(b) and $Cu_{0.72}Co_{2.24}O_4$(c) in 0.5 M Na_2SO_4 with 0.1 M KNO_3.

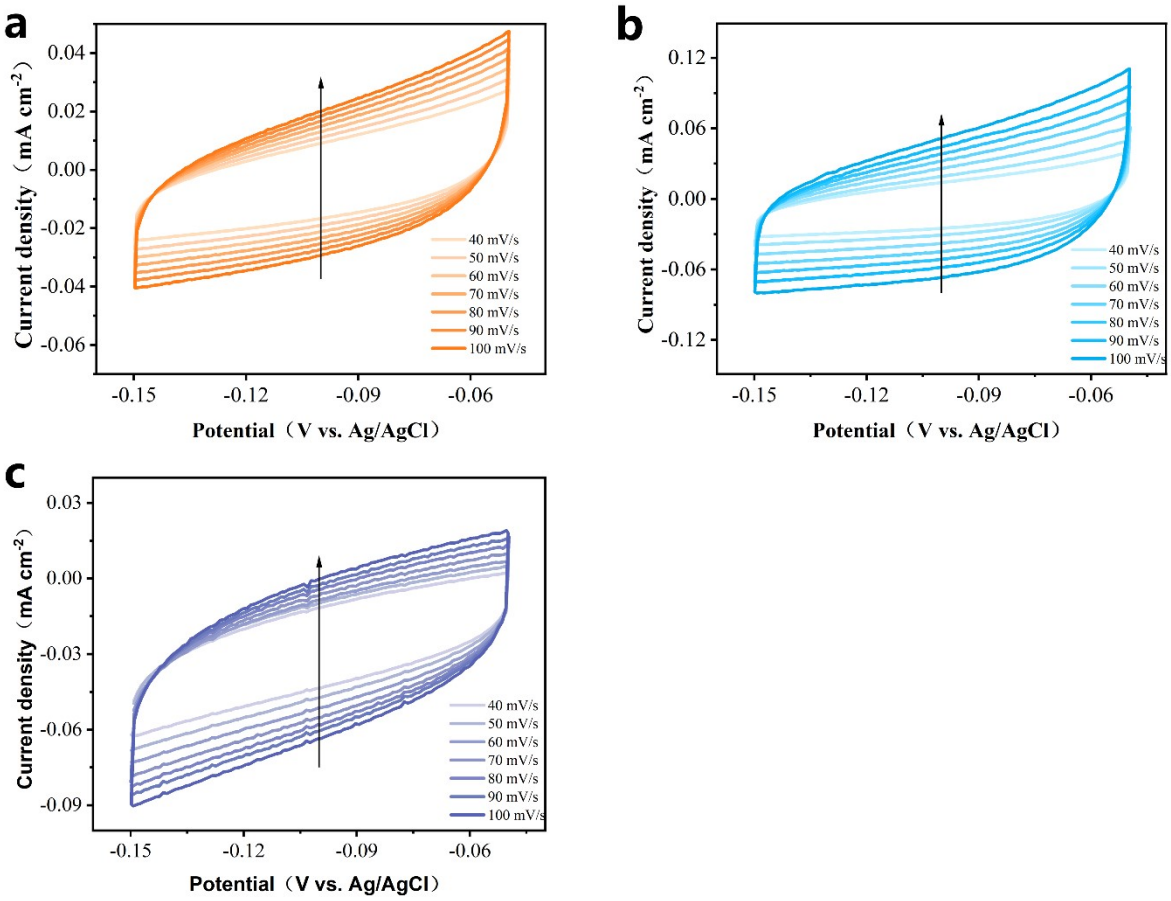

Figure S8. CV curves of CCOC (a), γ-$Cu_2(OH)_3Cl$ (b) and $Cu_{0.72}Co_{2.24}O_4$ (c) at varied scan rates (40 to 100 mV s-1) in the region of -0.05 to -0.15 V (vs. Ag/AgCl).

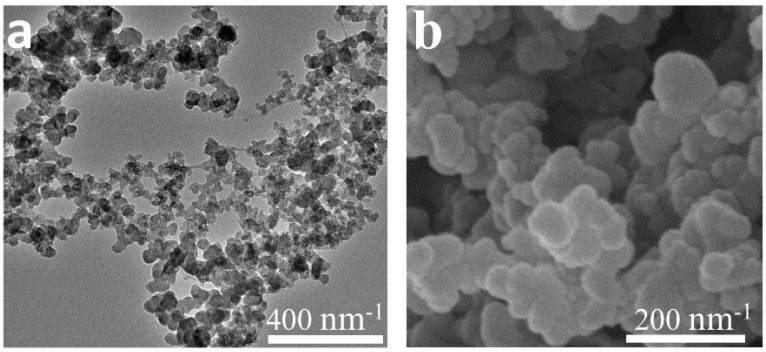

Figure S9. TEM (a) and SEM (b) images of CCOC after reaction for 5 h.

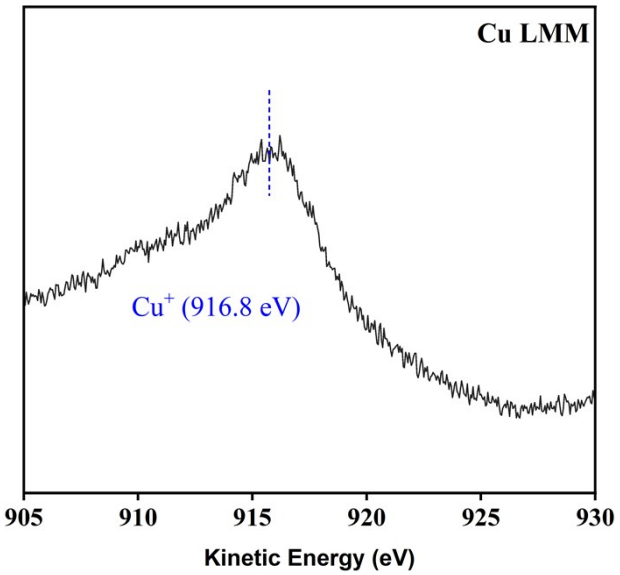

Figure S10. Cu LMM spectrum of CCOC after reaction for 2.5 h.

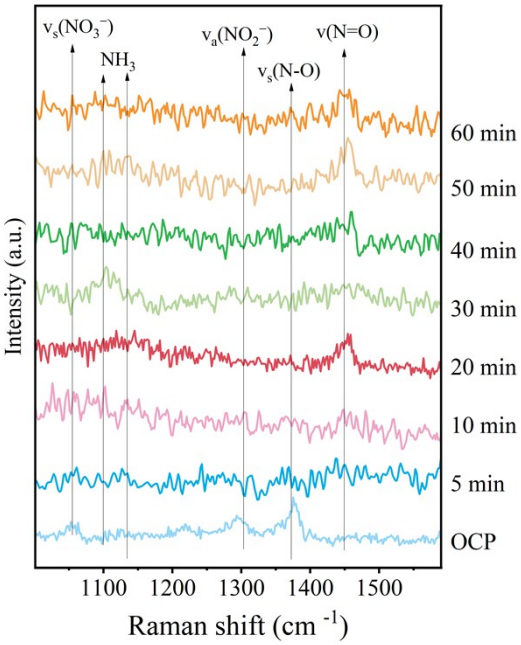

Figure S11. Electrochemical *in situ* Raman spectra of γ-$Cu_2(OH)_3Cl$ collected during NO_3^-RR from 0 to 60 min in Ar-saturated 0.5 M Na_2SO_4 with 0.1 M KNO_3.

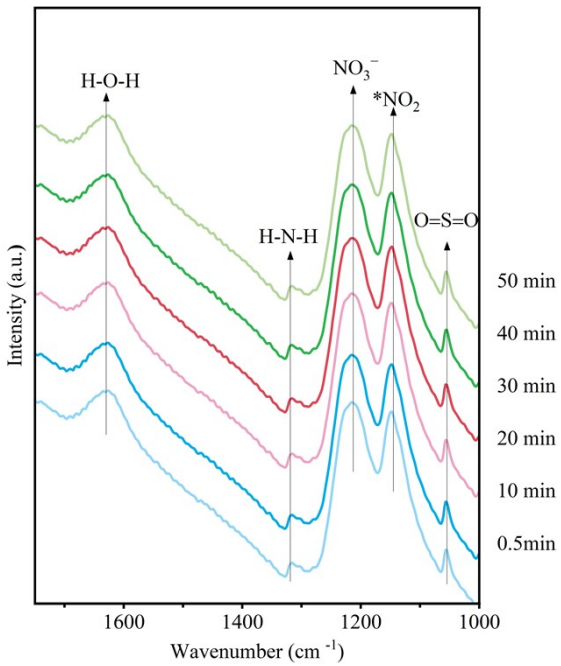

Figure S12. Electrochemical *in situ* FT-IR spectra of γ-$Cu_2(OH)_3Cl$ collected during eNO_3^-RR from 0 to 50 min in Ar-saturated 0.5 M Na_2SO_4 with 0.1 M KNO_3

Table S1. Mass ratio of Co and Cu in CCOC detected by ICP

	Wt%
Co	45.27
Cu	26.17

Table S2. Performance comparison of CCOC with previously reported electrocatalysts for NO_3^- RR.

Catalysts	Electrolyte	NH_3 yield	FE (%)	Reference
CCOC	**0.5 M Na_2SO_4 + 100 mM KNO_3**	**7.9 mg h^{-1} cm^{-2}**	**96**	**This work**
CCOC	**0.5 M Na_2SO_4 + 100 mM KNO_3**	**10.7 mg h^{-1} cm^{-2}**	**88**	**This work**
CuCoSP	1 M KOH + 100 mM KNO_3	19.9 mg h^{-1} cm^{-2}	93	[1]
CuCo/NC	0.2 M Na_2SO_4 + 200 mM $NaNO_3$	9.1 mg h^{-1} mg_{cat}^{-1}	95	[2]
Cu_1Co_1HHTP	0.5 M Na_2SO_4 + 100 mM $NaNO_3$	5.1 mg h^{-1} cm^{-2}	96	[3]
CuCoAl LDH	0.5 M PB+ 50 mM KNO_3	3.2 mg h^{-1} cm^{-2}	100	[4]
$CuCo_2O_4$/CFs	1 M KOH + 100 mM KNO_3	2.7 mg h^{-1} cm^{-2}	82	[5]
Cu-Co_3O_4/CC	0.1 M Na_2SO_4 + 35.7 mM KNO_3	6.2 mg h^{-1} mg_{cat}^{-1}	87	[6]
CoO/Cu foam	0.4 M Na_2SO_4 + 40 mM $NaNO_3$	4.3 mg h^{-1} cm^{-2}	97	[6]
Co_3O_4-$Cu_{2+1}O$/CF	0.5 M K_2SO_4 + 10 mM KNO_3	4.4 mg h^{-1} cm^{-2}	96	[7]
Cu_1-Fe	0.1 M K_2SO_4 + 35.7 mM KNO_3	~1.9 mg h^{-1} cm^{-2}	~90	[8]
PdCu SAA	0.5 M Na_2SO_4 + 9.7 mM $NaNO_3$	2.6 mg h^{-1} cm^{-2}	97.1	[9]
Mn-Cu NS	0.5 M K_2SO_4 + 10 mM KNO_3	4.3 mg h^{-1} cm^{-2}	95.8	[10]

Reference (SI)

[1] He, W., Zhang, J., Dieckhöfer, S., Varhade, S., Brix, A. C., Lielpetere, A., Seisel, S., Junqueira, J. R. C., & Schuhmann, W. (2022). Splicing the active phases of copper/cobalt-based catalysts achieves high-rate tandem electroreduction of nitrate to ammonia. *Nature Communications, 13*(1), 1129. doi:10.1038/s41467-022-28728-4

[2] Cheng, J., Dai, G., Sun, W., Yang, X., Xia, R., Xu, Y., & Mao, Y. (2024). Carbon Nanocage Confining CuCo Bimetallic Interface with Low Nitrate Adsorption Energy for Highly Efficient Electrochemical Ammonia Synthesis. *Energy & Fuels, 38*(3), 2501. doi:10.1021/acs.energyfuels.3c04371

[3] Liu, P., Yan, J., Huang, H., & Song, W. (2023). Cu/Co bimetallic conductive MOFs: Electronic modulation for enhanced nitrate reduction to ammonia. *Chemical Engineering Journal, 466*, 143134. doi:https://doi.org/10.1016/j.cej.2023.143134

[4] Wang, W., Chen, J., & Tse, E. C. M. (2023). Synergy between Cu and Co in a Layered Double Hydroxide Enables Close to 100% Nitrate-to-Ammonia Selectivity. *Journal of the American Chemical Society, 145*(49), 26678. doi:10.1021/jacs.3c08084

[5] Niu, Z., Fan, S., Li, X., Wang, P., Liu, Z., Wang, J., Bai, C., & Zhang, D. (2022). Bifunctional copper-cobalt spinel electrocatalysts for efficient tandem-like nitrate reduction to ammonia. *Chemical Engineering Journal, 450*, 138343. doi:https://doi.org/10.1016/j.cej.2022.138343

[6] Zhou, Y., Duan, R., Li, H., Zhao, M., Ding, C., & Li, C. (2023). Boosting Electrocatalytic Nitrate Reduction to Ammonia via Promoting Water Dissociation. *ACS Catalysis, 13*(16), 10846. doi:10.1021/acscatal.3c02951

[7] Zhang, J., Xu, D., Lu, D., & Wang, H. (2024). The synergistic tandem effect of Cu2+1O and Co3O4 enhances the activity and selectivity of nitrate reduction to ammonia in neutral solution. *Applied Catalysis A: General, 677*, 119695. doi:https://doi.org/10.1016/j.apcata.2024.119695

[8] Zhou, B., Yu, L., Zhang, W., Liu, X., Zhang, H., Cheng, J., Chen, Z., Zhang, H., Li, M., Shi, Y., Jia, F., Huang, Y., Zhang, L., & Ai, Z. (2024). Cu1−Fe Dual Sites for Superior Neutral Ammonia Electrosynthesis from Nitrate. *Angewandte Chemie International Edition, 63*(31), e202406046. doi:https://doi.org/10.1002/anie.202406046

[9] Du, C., Lu, S., Wang, J.-a., Wang, X., Wang, M., Fruehwald, H. M., Wang, L., Zhang, B., Guo, T., Mills, J. P., Wei, W., Chen, Z., Teng, Y., Zhang, J., Sun, C.-J., Zhou, H., Smith, R. D. L., Kendall, B., Henkelman, G., & Wu, Y. A. (2023). Selectively Reducing Nitrate into NH3 in Neutral Media by PdCu Single-Atom Alloy Electrocatalysis. *ACS Catalysis, 13*(16), 10560. doi:10.1021/acscatal.3c01088

[10] Wu, L., Jia, S., Zhang, L., Wang, R., Feng, J., Sun, X., & Han, B. (2024). Efficient nitrate electroreduction over Mn-doped Cu catalyst via regulating N-containing intermediates adsorption configuration. *Science China Chemistry,*

67(6), 1969. doi:10.1007/s11426-024-2040-8